INTERNATIONAL JOURNAL FOR NUMERICAL METHODS IN FLUIDS, VOL. 15, 233–245 (1992)

AN EFFICIENT PRESSURE–VELOCITY PROCEDURE FOR GAS–DROPLET TWO-PHASE FLOW CALCULATIONS

C. P. CHEN, H. M. SHANG AND Y. JIANG

Department of Chemical Engineering, University of Alabama in Huntsville, Huntsville, AL 35899, U.S.A.

SUMMARY

This paper presents a non-iterative numerical technique for computing time-dependent gas–droplet flows. The method is a fully interacting combination of Eulerian fluid and Lagrangian particle calculations. The interaction calculations between the two phases are formulated on a pressure–velocity-coupling procedure based on the operator-splitting technique. This procedure eliminates the global iterations required in the conventional particle-source-in-cell (PSIC) procedure. Turbulent dispersion calculations are treated by a stochastic procedure. Numerical calculations and comparisons with available experimental data as well as efficiency assessments are given for some sprays typical of spray combustion applications.

KEY WORDS Two-phase flow Pressure–velocity coupling Transient flow Turbulent dispersion

1. INTRODUCTION

Numerical modelling of two-phase turbulent reacting flows has practical applications in the development and design of many power-generating devices such as internal combustion engines and liquid rocket engines. In these flows, two-way coupling in terms of momentum, heat and mass transfer between underlying gas turbulence and dispersed spray droplets plays one of the most important physical roles of mixing and consequent spray combustion. In the last two decades computational techniques have been developed to characterize the dispersion of spray droplets in a gas and the influence of droplets on the gas dynamics. Generally there are two approaches commonly used to predict gas–droplet flows. In the first, called the 'two-fluid' model or Eulerian approach, the effect of two-way coupling is incorporated as extra source terms in the continuum equations for both phases. The advantage of using a continuum approach is its relatively high computational efficiency, especially for monodispersed systems.

Another approach, the so-called 'tracking' or Lagrangian approach, treats the particles as discrete entities in a turbulent flow field and their trajectories are calculated. This approach has the flexibility of handling polydispersed spray and the two-way couplings are usually accomplished through the particle-source-in-cell (PSIC) technique with exchange of momentum, heat and mass between the two phases. Both approaches have been studied extensively[1,2] and their comparative performances have also been investigated recently.[3,4] For typical spray combustion applications in which dense spray effects such as droplet collision, break-up and coalescence are important and drop dispersions are characterized by a non-uniform particle size distribution, the discrete particle approach is more convenient for representing the polydispersed spray.

In calculating turbulent gas–droplet flows, the most common discrete particle method is the stochastic separated flow approach as first described by Gosman and Ioannides[5] utilizing the

0271–2091/92/140233–13$11.50

Received 11 March 1991
Revised 23 October 1991

method of Crowe *et al.*[6] In this method the liquid spray droplets are represented by a finite number of computational parcels, a random sampling technique is entailed for instantaneous gas flow properties based on a specified turbulence model and the resulting fluctuations are used in a Lagrangian computation for parcel motion. The mutual coupling between gas and droplets is accounted for by estimating the particle source term for each computational cell visited by the droplets. This is followed by a recalculation of the flow field incorporating these source terms. Thus a global itevative process (in addition to the iterations within the gas flow solution procedure) between the continuous phase solver and the droplet equation of motion are required.[7] This method has been used primarily for statistically steady flows.[2,8,9] For transient problems this global iteration at each time step can introduce such excessive computational requirements that numerical simulation becomes impractical. Dukowicz[10] has introduced a time-splitting method to couple the gas–particle interactions in a transient calculation. The numerical scheme used in his method is based on the SOLA code, which utilizes a pressure substitution scheme. A similar time-splitting method has been used by Raju and Sirignano[11] in a pressure correction scheme for steady state calculations and by Sabnis and de Jong[12] in a density-based scheme. Recently the method of Dukowicz has been extended by O'Rourke[13] into a comprehensive computer code KIVA-II.[14] The numerical scheme used in the KIVA-II code is based on the ALE-ICE scheme, which uses an iterative procedure similar to the SIMPLE algorithm for pressure corrections in the ICE. In these newer methods the two-phase coupling procedures are still iterative in nature at each time step for transient calculations.

The main effort of this paper is to present a numerical method for coupling the gas–droplet interactions using a newly developed pressure correction scheme.[15] This method utilizes the operator-splitting technique in deriving a predictor–multicorrector sequence which eliminates the global iteration between the two phases at each time step. The method of Reference 15 reduces to the PISO algorithm of Issa[16] for single-phase incompressible flow calculations. We have found that the present two-phase method is efficient and that the required number of computational parcels to achieve satisfactory accuracy is also not excessive. In the following sections, formulations and validations of this method are presented.

2. NUMERICAL MODEL

The gas flow was formulated using the Eulerian conservation equations of mass and momentum. The spray is described by the discrete particle method formulated on a Lagrangian frame. The spray is assumed to be sufficiently dispersed (no collision between droplets) and for simplicity the gas flow is assumed to be close to incompressible. The governing equations are as follows.

Gas phase

$$\frac{\partial \rho}{\partial t}+\frac{\partial}{\partial x_i}(\rho U_i)=\dot{S}^m, \tag{1}$$

$$\frac{\partial \rho U_i}{\partial t}+\frac{\partial}{\partial x_i}(\rho U_i)=-\frac{\partial P}{\partial x_j}-\frac{\partial}{\partial x_j}(\Gamma_{ij})+\bar{F}_i. \tag{2}$$

Here all variables are ensemble-averaged mean quantities and

$$\Gamma_{ij}=-(\mu+\mu_t)\left[\frac{1}{2}\left(\frac{\partial U_i}{\partial x_j}+\frac{\partial U_j}{\partial x_i}\right)\right]+\tfrac{2}{3}\delta_{ij}k, \tag{3}$$

in which μ_t is the eddy viscosity.

Particle phase

$$\frac{\mathrm{d}x_i}{\mathrm{d}t} = v_i, \tag{4}$$

$$\frac{\mathrm{d}v_i}{\mathrm{d}t} = F_{pi} + g_i. \tag{5}$$

Equation (5) represents a form in which the virtual mass term, Basset term and pressure gradient term have been neglected from the full BBO (Boussinesq–Basset–Oseen) equation. For cases of interest in most spray combustion applications, i.e. $\rho \ll \rho_\mathrm{d}$, dimensional analysis justifies the simplification of equation (5).

Since the formulation here is essentially a statistical approach, each computational parcel represents a large number of droplets having equal location, velocity, size and temperature. The two-way coupling between the two phases is accounted for by the interaction terms, where

$$F_{pi} = \frac{U_i + u_i' - v_i}{\tau}, \tag{6}$$

$$\dot{S}^m = \sum_{p=1}^{NP} N_p \dot{m}_{\mathrm{ev},p}/\mathrm{d}V \tag{7}$$

for evaporating spray;[17]

$$F_i = \sum_{p=1}^{NP} \left[N_p \dot{m}_{\mathrm{ev},p} (v_i)_p - \tfrac{4}{3}\pi \rho_\mathrm{d} r_p^3 N_p \left(\frac{\mathrm{d}v_i}{\mathrm{d}t} \right)_p \right] \Big/ \mathrm{d}V, \tag{8}$$

in which $\mathrm{d}V$ denotes the computational cell and the effective relaxation time is given as $\tau = t_*/f$, with $t_* = \rho_\mathrm{d} d_p^2/18\mu$ and $f = C_\mathrm{D} Re_p/24$. The form of C_D is given in the Appendix. Other details of interaction mechanisms such as mass transfer rate and heat transfer rate as well as energy equations for both phases can be found in Reference 17, in which the physical aspects of our method are described.

It suffices here to illustrate the calculation method for the non-evaporating case ($\dot{m}_{\mathrm{ev},p} = 0$). The method is based on the operator-splitting technique, attempting to reach an accurate transient solution after prescribed predictor–corrector steps for each time-marching step. The generalization of this operator-splitting technique for deriving pressure correction equations suitable for all-speed flows is described separately.[15,18] We focus in this paper on the coupling of the dispersed phase in the solution procedure.

Discretization of the gas phase governing equation uses the finite volume approach. Differencing in the temporal domain employs the implicit Euler scheme. All the dependent and independent variables are stored at the same grid location and the variables at the finite control volume boundaries are interpolated between adjacent grid points. The discretizations have been performed on a general non-orthogonal curvilinear co-ordinate system with a second-order upwind scheme for convection terms and the central differencing scheme for diffusion terms.[19] The resulting discretized equations were solved by a conjugate gradient (CGS) solver.[19]

For the incompressible gas flows considered here, the pressure–velocity coupling between the momentum and continuity equations is an important issue, since the density is constant. In the pressure correction method the derivation of the pressure equation, which includes the effect of droplets, plays a key role in determining whether the velocity field satisfies the local mass continuity equation. In this study a non-iterative operator-splitting algorithm following the spirit of References 16 and 18 is used to derive a predictor–corrector sequence. We seek the finite

difference form of the governing equations (2) and (5) as follows:

$$\left(\frac{\rho}{\Delta t}-A_0\right)U_i^{n+1}=H'(U_i^{n+1})-\Delta_i P^{n+1}+S_i+\bar{F}_i^{n+1}, \tag{9}$$

$$\frac{v_i^{n+1}-v_i^n}{\Delta t}=\frac{U_i^{n+1}+u_i'-v_i^{n+1}}{\tau^{**}}+g_i. \tag{10}$$

The effective relaxation time scale τ is evaluated at the second corrector level (**), to be defined later. The superscripts n and $n+1$ denote time levels t^n and t^{n+1} respectively. Operators A_0 and $H'(\ )$ are constructed from the second-order upwind scheme for the convection terms and the central differencing scheme for the diffusion terms respectively and S_i is the source term associated with the Cartesian mean velocity component.[18,19] It has been shown in Reference 10 that the ensemble-averaged interaction term $\bar{F}_i$ can be replaced by volume averaging. We split this term as

$$\bar{F}_i^{n+1}=-S_u^{**}U_i^{n+1}+R_u^{**}, \tag{11}$$

in which S_u^{**} and R_u^{**} are obtained by rearranging equation (10):

$$S_u^{**}=\frac{1}{\mathrm{d}V}\sum_p^{NP}N_p m_p/(\Delta t+\tau_p^{**}), \tag{12}$$

$$R_u^{**}=\frac{1}{\mathrm{d}V}\sum_p^{NP}N_p m_p/(\Delta t+\tau_p^{**})(v_i^n-u_i'+g_i\tau_p^{**})_p, \tag{13}$$

where $m_p=\frac{4}{3}\pi r_p^3\rho_d$ is the particle mass. The parameters S_u^{**} and R_u^{**} are momentum control volume quantities depending on the available particle information at the second corrector level to be discussed later.

By the operator-splitting method we divide the predictor–corrector procedure as follows.

For the predictor step

$$\left(\frac{\rho}{\Delta t}-A_0\right)U_i^*=H'(U_i^*)-\Delta_i P^n+S_i-S_u^nU_i^*+R_u^n, \tag{14}$$

$$\frac{v_i^*-v_i^n}{\Delta t}=g_i+\frac{U_i^*+(u_i')^n-v_i^*}{\tau^n}. \tag{15}$$

The quantities S_u^n and R_u^n are determined from the existing flow fields. These values of U_i^* and v_i^* are used to evaluate τ^*, S_u^* and R_u^* such that a second approximation to the gas velocities can be performed:

$$\left(\frac{\rho}{\Delta t}-A_0\right)U_i^{*T}=H'(U_i^*)-\Delta_i P^n+S_i-S_u^*U_i^{*T}+R_u^*. \tag{16}$$

By subtracting (14) from (16), we also obtain the velocity correction equation

$$\left(\frac{\rho}{\Delta t}-A_0\right)(U_i^{*T}-U_i^*)=-S_u^*U_i^{*T}+S_u^nU_i^*+R_u^*-R_u^n. \tag{17}$$

For the first corrector step the momentum equation is approximated by

$$\left(\frac{\rho}{\Delta t}-A_0\right)U_i^{**}=H'(U_i^{*T})-\Delta_i P^*+S_i-S_u^*U_i^{**}+R_u^*. \tag{18}$$

Subtracting (17) from (18) gives

$$\left(\frac{\rho}{\Delta t}-A_0+S_u^*\right)(U_i^{**}-U_i^{*T})=H'(U_i^{*T}-U_i^*)-\Delta_i(P^*-P^n). \tag{19}$$

Taking the divergence of (19) and invoking continuity ($\nabla U_i^{**}=0$), the pressure correction equation is obtained as

$$\Delta_i[D_u^*\Delta_i(P^*-P^n)]=\Delta_i U_i^{*T}+\Delta_i[D_u^*H'(U_i^{*T}-U_i^*)]. \tag{20}$$

Here we have used the short notation $D_u^*=(\rho/\Delta t-A_0+S_u^*)^{-1}$. The particle momentum at this level is then

$$\frac{v_i^{**}-v_i^n}{\Delta t}=g_i+\frac{U_i^{**}+(u_i')^n-v_i^{**}}{\tau^*}. \tag{21}$$

The values obtained at this level are used to calculate τ^{**}, S_u^{**} and R_u^{**} and to further update the velocities for the gas phase,

$$\left(\frac{\rho}{\Delta t}-A_0\right)U_i^{**T}=H'(U_i^{*T})-\Delta_i P^*+S_i-S_u^{**}U_i^{**T}+R_u^{**}, \tag{22}$$

or the velocity correction equation ((22) minus (18)),

$$\left(\frac{\rho}{\Delta t}-A_0\right)(U_i^{**T}-U_i^{**})=-S_u^{**}U_i^{**T}+S_u^*U_i^{**}+R_u^{**}-R_u^*. \tag{23}$$

At this stage the mean velocity field satisfies the continuity constraint. To further satisfy the momentum conservation, a second corrector step is used:

$$\left(\frac{\rho}{\Delta t}-A_0\right)U_i^{***}=H'(U_i^{**T})-\Delta_i P^{**}+S_i-S_u^{**}U_i^{***}+R_u^{**}. \tag{24}$$

By subtracting (22) from (24), taking the divergence and invoking continuity again, we obtain the following pressure correction and velocity correction equations:

$$\Delta_i[D_u^{**}\Delta_i(P^{**}-P^*)]=\Delta_i U_i^{**T}+\Delta_i[D_u^{**}H'(U_i^{**T}-U_i^{*T})], \tag{25}$$

$$\left(\frac{\rho}{\Delta t}-A_0+S_u^{**}\right)(U_i^{***}-U_i^{**T})=H'(U_i^{**T}-U_i^{*T})-\Delta_i(P^{**}-P^*). \tag{26}$$

Following Reference 16, it can be shown that the errors introduced by the operator-splitting procedure are less than the truncation errors of the finite difference scheme used in the governing equations (9) and (10). Note that the effective relaxation time τ depends on the drag function, which should contain the effects of turbulence. Here the two important aspects of turbulence–droplet interactions,[3] namely the turbulent droplet dispersion and the turbulence modulation effects, can be included. Owing to the dilute spray assumption used in this study, the modulation effect is neglected.[1,3] The turbulence dispersion effect is accounted for by the Monte Carlo procedure utilizing the k–ε two-equation model. Physical aspects of this procedure are discussed extensively in the literature.[1–4,8,17] Computationally, we need to calculate $(u_i')^*$ at this stage by using the newly updated values of turbulence kinetic energy and its dissipation rate. A one-predictor (implicit)/one-correction (explicit) procedure for the k- and ε-equations suggested by Issa[16] (see also Reference 18) has been used in this study. We then let U_i^{***} and P^{**} be the values at level t^{n+1} and add $(u_i')^*$ to update the final-time-level particle velocities using the

equation

$$\frac{v_i^{n+1}-v_i^n}{\Delta t}=\frac{U_i^{n+1}+(u_i')^*-v_i^{n+1}}{\tau^{**}}+g_i. \tag{27}$$

This brings all variables to the new time level. The time is then incremented and the new predictor–corrector sequence is repeated with the new velocities. This algorithm is used for the simulation of transient phenomena. If only a statistically steady solution is desired, the time steps for the gas phase and particle phase can be made unequal; also, the U_i^{*T} and U_i^{**T} calculation steps can be neglected.

3. NUMERICAL APPLICATIONS

The above proceedures have been coded into the MAST (multiphase all-speed transient flow solver) programme for various two-phase flow calculations. We first present the solid particle dispersion calculation in nearly homogeneous turbulence to calibrate the stochastic simulation of particle–turbulence interactions.

Discrete phase turbulent dispersion

The stochastic technique used for modelling the discrete phase turbulent dispersion is similar to the methods used by, for example, Dukowicz,[10] Gosman and Ioannides[5] and Shuen *et al.*[20] The continuous phase turbulence is assumed to be isotropic and the random turbulent velocity components u_i' are assumed to have a Gaussian probability distribution with standard deviation $(2k/3)^{1/2}$. The u_i' at any required location is then obtained by randomly sampling the distribution and changes discontinuously after each passage of the droplet–turbulence interaction time t_{int}. The time t_{int} corresponds physically to an eddy lifetime t_e or to a time t_{tr} for a particle to traverse a typical turbulent eddy. In References 3, 5, 10 and 20 different formulations for choosing t_e, t_{tr} and t_{int} are proposed. Here we choose $l_e=1{\cdot}65\,C_\mu^{3/4}k^{3/2}/\varepsilon$ for the characteristic size of an eddy and $t_e=3C_\mu k/\varepsilon$ for the eddy lifetime to match the asymptotic dispersion analysis of Hinze.[21]

The particle dispersion experimental set-up of Snyder and Lumley[22] in a grid-generated turbulent flow was used for the numerical model validation. Particle densities and sizes are chosen to examine the phenomena in which the eddy lifetime controls interaction times (46·5 μm diameter hollow glass), the transit time controls interaction times (87·0 μm corn pollen) or the interaction-controlling time undergoes a transition from transit time to eddy lifetime (87·0 μm solid glass). In this experiment fluid turbulence intensities and length scale information were measured. These measured value were used here; thus the k–ε model was not solved for this calculation. The particle calculations were started at the experimental particle injection point $x/m=20$ (m is a 2·54 cm × 2·54 cm square mesh). The particle velocity was assumed equal to the mean fluid velocity of 6·55 m s^{-1}. 5000 computational particles were sampled to calculate the resulting mean square dispersion with respect to time.

Comparison of the predicted and measured particle dispersions is shown in Figure 1. The agreement is considered quite good. The comparison here is more favourable compared with previous calculations by Shuen *et al.*[20] and Gosman and Ioannides,[5] especially for medium particles for which the controlling particle–turbulence interaction time goes through a transition from t_e to t_{tr}. In this study we do not estimate t_{int} as suggested in Reference 20, where t_{tr} was calculated from a simplified BBO equation without the gravity effect. Instead we follow the stochastic procedure suggested by Nichols[23] and trace particle trajectories as time progresses. This method has the flexibility of taking into account both the gravity effect (crossing trajectory effect) and the non-Stokesian drag law and gives more satisfactory results for medium particles.

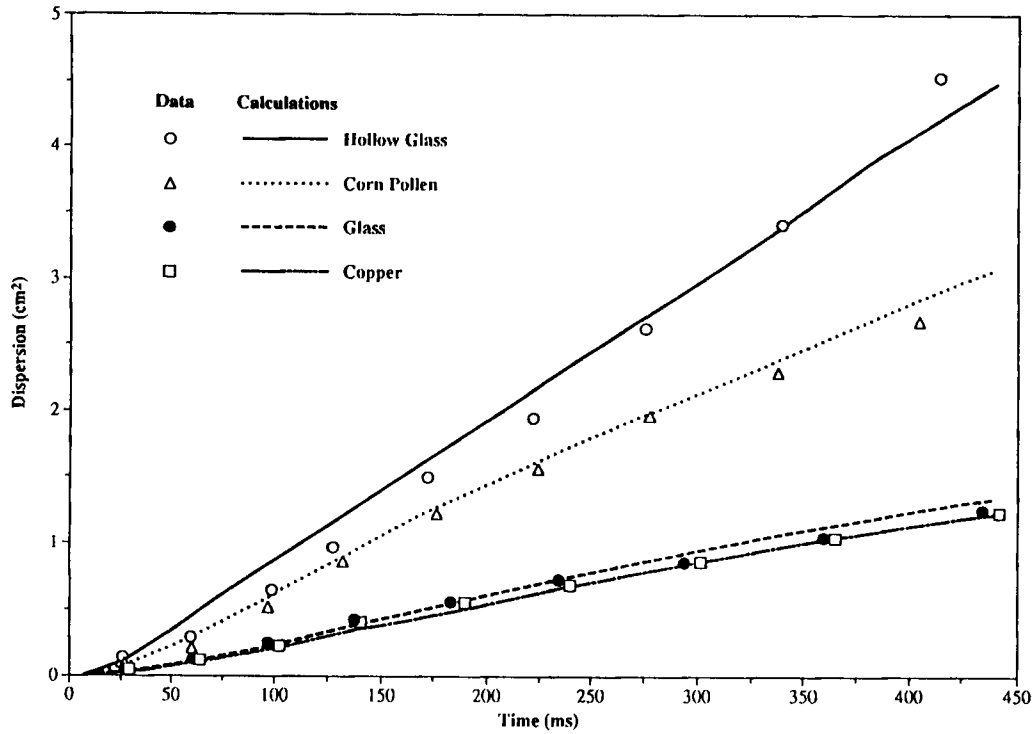

Figure 1. Particle dispersion in a grid-generated turbulent flow

Single-fuel-injector case

The experiments of Hiroyasu and Kadota[24] are used to validate the transient non-evaporating spray calculations. To rigorously model this flow, detailed atomization processes have to be resolved at the injector nozzle. Since this phenomenon is not modelled in this study, information about the injected droplet size distribution as well as the velocity distribution has to be estimated in the vicinity of the injector at which the calculation starts. Following the suggestions of Dukowicz,[10] the initial particle injection velocity was determined by the mass flow rate and pressure difference of the nozzle. The estimated initial spray angle was also guided by Dukowicz.[10] The initial particle size distribution was given by the following form:

$$f_d(d_p) = \frac{6}{D_{32}} \exp\left(\frac{-3d_p}{D_{32}}\right),$$

where D_{32} is the Sauter mean diameter.

The test conditions are given in Table I. The spray was assumed to be axially symmetric and the calculation was carried out in cylindrical co-ordinates. The computed penetration of the tip of the spray as a function of time for the two test conditions is shown qualitatively in Figure 2 and compared quantitatively with the experimental data in Figure 3. The comparison is very good here. Although the initial jet penetration depends greatly on the assumed initial spray condition, the consequent good prediction at the later time demonstrates the accuracy of the numerical scheme and importance of the droplet–gas interaction.

Table I. Single-orifice injection parameters[24]

Chamber gas pressure (atm)	Injection velocity ($m\,s^{-1}$)	Gas density ($kg\,m^{-3}$)	Mass flow rate ($kg\,s^{-1}$)	Sauter mean radius (SMR) (μm)	Nozzle pressure difference ΔP (atm)
1	122·2	1·123	0·00726	5·0	98
30	102·5	33·70	0·00609	5·0	69

Fuel: diesel fuel oil, $\rho_d = 840\,kg\,m^{-3}$.
Ambient gas: nitrogen.
Nozzle diameter: 0·3 mm.

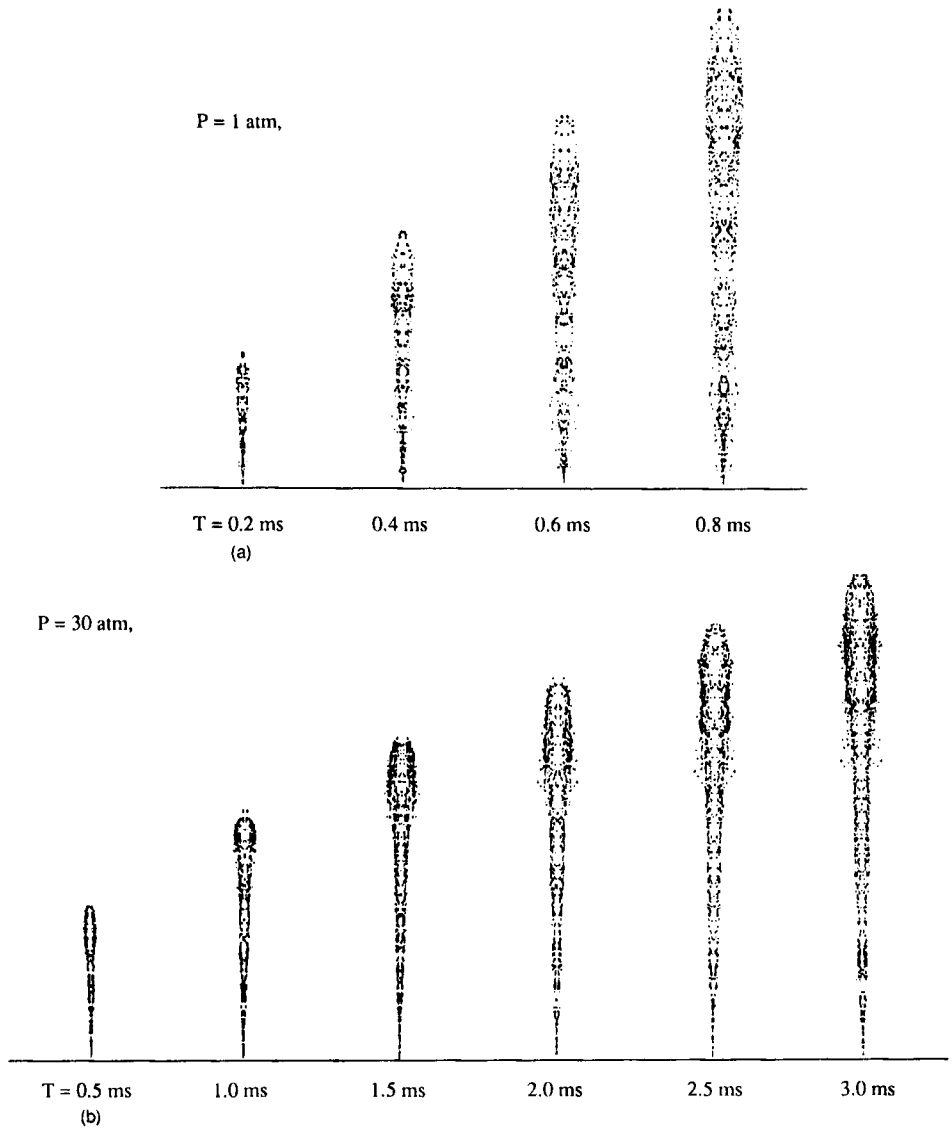

Figure 2. Particle plots of a single-orifice spray

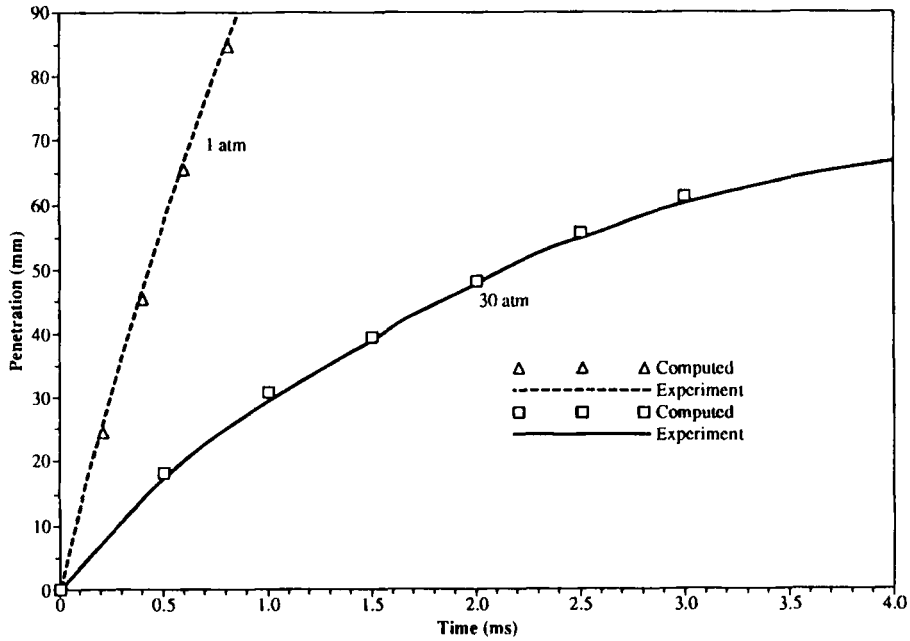

Figure 3. Comparison of computed spray penetration with experimental data[24]

Table II. Hollow cone spray parameters

Chamber gas pressure (atm)	Injection velocity ($m\,s^{-1}$)	Injection angle (deg)	Gas density ($kg\,m^{-3}$)	Mass flow rate ($kg\,s^{-1}$)	Sauter mean radius (SMR) (μm)
1	20·0	30	1·123	4×10^{-4}	2·5

Table III. Efficiency assessment

	MAST 2D		TEACH/PSIC	
	Particles	CPU time (s)	Particles	CPU time (s)
Single-orifice spray				
41 × 61 grid	600	126·9	800	1420
300 time steps	1200	135·7		
Hollow cone spray				
31 × 31 grid	400	74·9	800	934
200 time steps	1000	88·3		

Hollow cone spray

A polydispersed, pulsed, hollow cone spray case of practical importance is also chosen for the test conditions listed in Table II. Figure 4 shows the particle plot and the gas velocity vectors for a 30° spray. With a back pressure of 1 atm the interaction between the gas and droplets is seen to be rather strong. The shape of the spray is no longer conical even for very short times and the spray penetration is suppressed by the interaction of the droplets with the induced air flow. The gas velocity vectors indicate the presence of a vortex near the head of the spray, which curls the spray tip towards the outside of the spray. A substantial region of strong inward flow in the centre of the

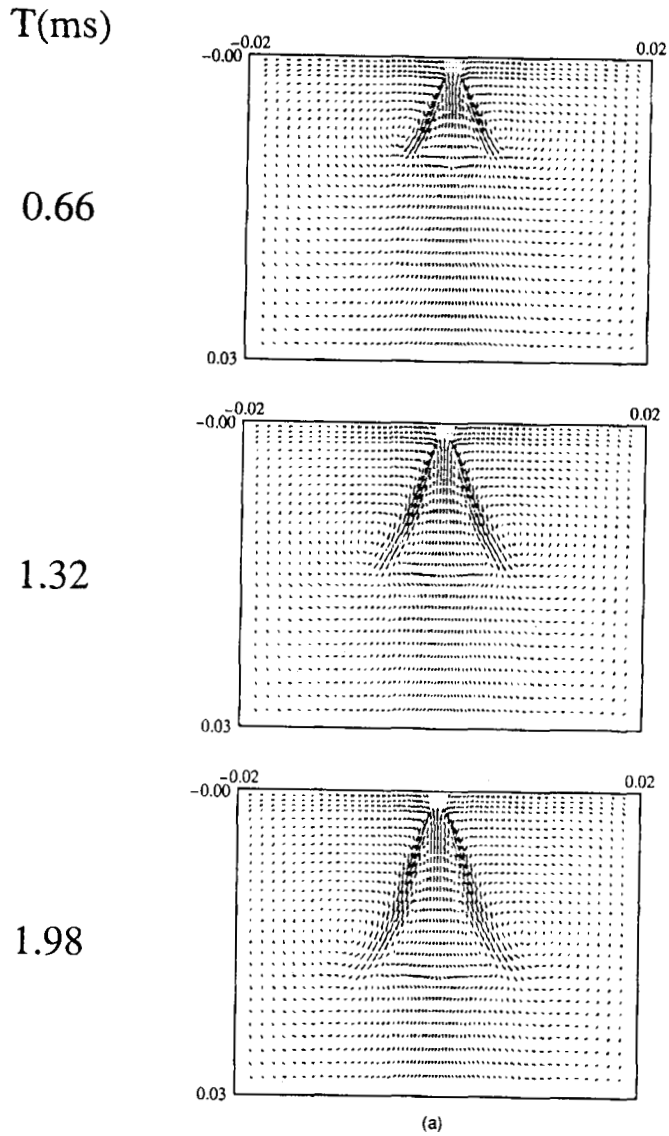

Figure 4. (a) Velocity vectors and (b) particle plot of a 30° hollow cone spray

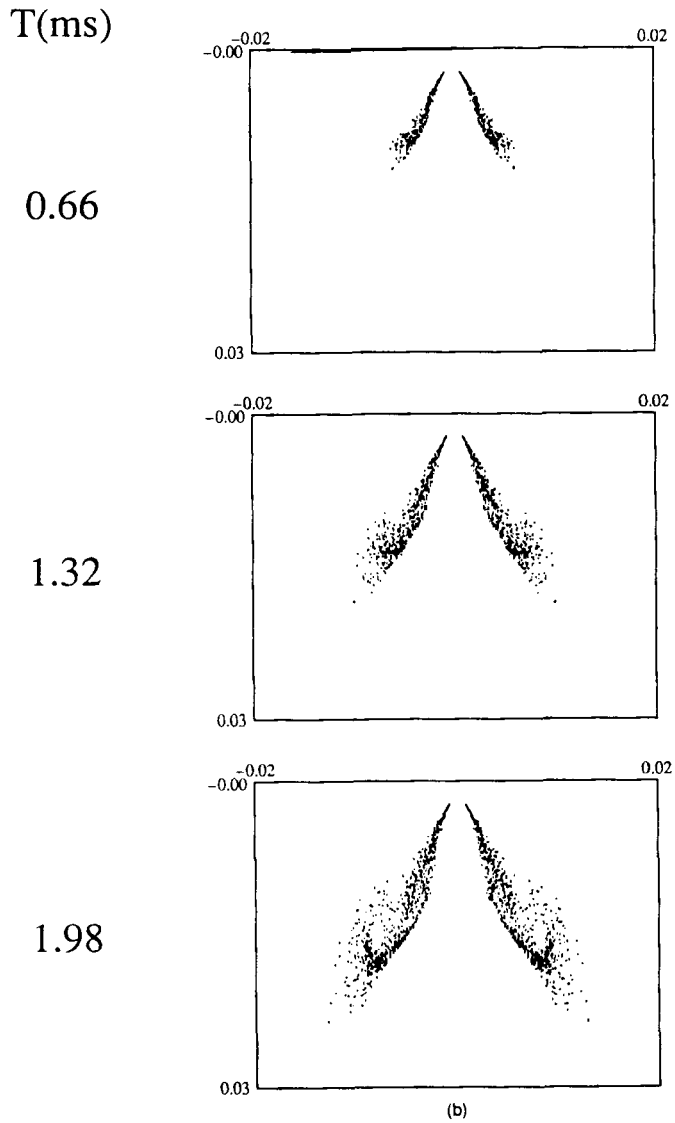

Figure 4. (Continued)

cone near the injector was also observed. These flow patterns and spray shapes compare quite favourably with experimental observations.[25]

The efficiency assessment of the present numerical method is shown in Table III for the single-orifice and hollow cone spray cases. The CPU times on a CRAY X/MP using the MAST code with the present method and the TEACH code with the PSIC method[3] for both transient spray calculations with $\Delta t = 0{\cdot}1$ ms are given. It can be seen that the amount of CPU time is reduced by about one order of magnitude using the present calculation procedure. Also, the present method is rather independent of particle number. This is due to the fact that particles are injected at each time step and the source terms in the continuous phase are updated for all the particles at each

Eulerian control volume, while in the TEACH/PSIC method all the particles have to be tracked and the continuous phase flow field is held frozen between the global iterations at each time step. This PSIC algorithm thus requires substantial computer time and is inherently unsuitable for transient calculations.

4. CONCLUSIONS

A new numerical scheme based on a non-iterative predictor–corrector pressure–velocity-coupling procedure has been developed for transient gas–droplet two-phase flows. The present scheme is formulated on a Eulerian–Lagrangian analysis and the two-way interaction between the two phases is handled through a strong coupling procedure. This procedure eliminates global iterations conventionally used in the PSIC procedure and shows drastic savings in CPU time for transient spray calculations. This method has recently been extended to evaporating spray calculations.[17] Good agreements between the calculated results and the experimental data have been obtained despite the uncertainties in the inlet conditions for both fluid and droplets. The development of the technique is based on the assumption of dilute (non-iterating) sprays. The computer code, however, allows easy alteration of models, so that an appropriate model to suit the physical problem of interest can be quickly implemented. Experimental studies with better defined inlet conditions would be extremely useful in further model validations.

ACKNOWLEDGEMENTS

This study is supported by NASA grant (NAG8-092 and partially by NAG8-128). The authors wish to acknowledge the CRAY CPU time supplied by the Alabama Supercomputer Network through UAH.

APPENDIX: NOMENCLATURE

C_D	drag coefficient
C_μ	model constant for k–ε model, $C_\mu = 0{\cdot}09$
d_p	droplet diameter for computational particle p
f	$C_D Re_p/24$; $f=1$ for $Re_p \leq 1$, $f = 1 + 0{\cdot}15\ Re_p^{0{\cdot}687}$ for $Re_p > 1$
F_i	interaction force due to droplets
F_{pi}	particle drag force
g_i	gravity vector
k	kinetic energy
N_p	number of droplets for each computational particle p
NP	number of computational particles
P	mean pressure
r_p	droplet radius
Re_p	particle Reynolds number; $Re_p = \rho d_p \lvert U_i + u_i' - v_i \rvert / \mu$
S_i	source terms in momentum equation
t_e	eddy lifetime
t_{int}	droplet–turbulence interaction time
t_{tr}	particle transit time
t_*	particle relaxation time, $t_* = \rho_d d_p^2/18\mu$
u_i	instantaneous velocity for gases, $u_i = U_i$ (mean) $+ u_i'$ (fluctuation)
v_i	instantaneous velocity for droplets

Greek letters

τ	effective particle relaxation time
ρ	fluid (gas) density
ρ_d	droplet density
μ	gas viscosity
ε	dissipation rate of turbulent kinetic energy

REFERENCES

1. G. M. Faeth, 'Mixing, transport and combustion in sprays', *Prog. Energy Combust. Sci.*, **13**, 293–345 (1987).
2. R. S. L. Lee and F. Durst (eds), *Proc. Int. Conf. on Mechanics of Two-phase Flows*, Taipei, 1989.
3. A. Fashola, and C. P. Chen, 'Modeling of confined turbulent fluid–particle flows using Eulerian and Lagrangian schemes', *Int. J. Heat and Mass Transfer*, **33**, 691–700 (1990).
4. A. A. Mostafa and H. C. Mongia, 'On the modeling of turbulent evaporating sprays: Eulerian versus Lagrangian approach', *Int. J. Heat Mass Transfer*, **30**, 2583–2593 (1987).
5. A. D. Gosman and E. Ioannides, 'Aspects of computer simulation of liquid-fueled combusters', *AIAA Paper 81-0323*, 1981.
6. C. T. Crowe, M. P. Sharma and D. E. Stock, 'The particle-source-in cell (PSI-cell) model for gas–droplet flows', *J. Fluid Eng.*, **99**, 325–332 (1977).
7. F. Durst, D. Milojevic and B. Schonung, 'Eulerian and Lagrangian predictions of particulate two-phase flows: a numerical study', *Appl. Mech. Model.*, **8**, 101–115 (1984).
8. J. P. Ashiem and J. E. Peters, 'Alternative fuel spray behavior', *J. Propul. Power*, **5**, 391–398 (1989).
9. J. Boysan, W. H. Ayers and K. Swithenbank, 'A fundamental modeling approach to cyclone design', *Trans. IChemE*, **60**, 222–230 (1982).
10. J. K. Dukowicz, 'A particle–fluid numerical model for liquid sprays', *J. Comput. Phys.*, **35**, 229–253 (1980).
11. M. S. Raju and W. A. Sirignano, 'Multicomponent spray computations in a modified centerbody combuster', *J. Propul. Power*, **6**, 97–105 (1990).
12. J. S. Sabnis and F. J. de Jong, 'Calculation of the two-phase flow in an evaporating spray using an Eulerian–Lagrangian analysis', *AIAA Paper 90-0447*, 1990.
13. P. J. O'Rourke, 'Statistical properties and numerical implementation of a model for droplet dispersion in a turbulent gas', *J. Comput. Phys.*, **83**, 345–360 (1989).
14. A. A. Amsden, P. J. O'Rourke and T. D. Butler, 'KIVA-II: a computer program for chemically reactive flows with spray', *Los Alamos National Laboratory Rep. LA-11560-MS*, May 1989.
15. Y. Jiang, C. P. Chen and H. M. Shang, 'A new pressure–velocity coupling procedure for inviscid and viscous flows at all speeds', *Proc. 4th Int. Symp. on Computational Fluid Dynamics*, Davis, CA, September 1991, pp. 545–550.
16. R. I. Issa, 'Solutions of the implicitly discretized fluid flow equations by operator-splitting', *J. Comput. Phys.*, **62**, 40 (1985).
17. H. M. Shang, C. P. Chen and Y. Jiang, 'Turbulence modulation effect on evaporating spray characterization', *AIAA Paper 90-2442*, 1990.
18. C. P. Chen, Y. Jiang and H. M. Shang, 'MAST—a computer code for multiphase all-speed transient flows', *NASA NAG8-092*, 1990.
19. Y. Jiang, C. P. Chen and P. K. Tucker, 'Multigrid solution of unsteady Navier–Stokes equations using a pressure method', *Numer. Heat Transfer, Part A*, **20**, 81–93 (1991).
20. J. S. Shuen, L. D. Chen and G. M. Faeth, 'Evaluation of a stochastic model of particle dispersion in a turbulent round jet', *AIChE J.*, **29**, 167–170 (1983).
21. J. O. Hinze, *Turbulence*, 2nd edn, McGraw-Hill, New York, 1975, Chap. 5.
22. W. H. Snyder and J. L. Lumley, 'Some measurements of particle velocity autocorrelation functions in a turbulent flow', *J. Fluid. Mech.*, **48**, 41–71 (1971).
23. R. H. Nichols, 'The effect of particle dynamics on turbulence measurements with the laser velocimeter', in *Numerical Methods for Multiphase Flows, ASME FED, Vol. 91*, ASME, New York, 1990, pp. 35–45.
24. H. Hiroyasu and T. Kadota, 'Fuel droplet size distribution in diesel combustion chamber', *SAE Paper 740715*, 1974.
25. K. Meintjes, 'Engine combustion modeling: prospects and challenges', *Cray Channels*, Winter issue, 12–15 (1987).